Heliyon

Received:
20 February 2018
Revised:
4 August 2018
Accepted:
24 September 2018

Cite as: Zahir Shah, Ebenezer Bonyah, Saeed Islam, Waris Khan, Mohammad Ishaq. Radiative MHD thin film flow of Williamson fluid over an unsteady permeable stretching sheet.
Heliyon 4 (2018) e00825.
doi: 10.1016/j.heliyon.2018.e00825

Radiative MHD thin film flow of Williamson fluid over an unsteady permeable stretching sheet

Zahir Shah [a], **Ebenezer Bonyah** [b,*], **Saeed Islam** [a], **Waris Khan** [c], **Mohammad Ishaq** [c]

[a] *Department of Mathematics, Abdul Wali Khan University, Mardan, Khyber Pakhtunkhwa 23200, Pakistan*

[b] *Department of Information Technology Education, University of Education Winneba-(Kumasi Campus), Kumasi 00233, Ghana*

[c] *Department of Mathematics, Islamia College University, Peshawar, Khyber Pakhtunkhwa 25000, Pakistan*

[*] Corresponding author.

E-mail address: ebbonya@gmail.com (E. Bonyah).

Abstract

In this research work we have examined the flow of Williamson liquid film fluid with heat transmission and having the impact of thermal radiation embedded in a permeable medium over a time dependent stretching surface. The fluid flow of liquid films is assumed in two dimensions. By using suitable similarity transformation the governing non-linear partial differential equations have been transformed into non-linear differential equations. An optimal approach has been used to acquire the solution of the modelled problem. The convergence of the technique has been shown numerically. The impact of the Skin friction and Nusslet number and their influence on thin film flow are shown numerically. Thermal radiation, unsteadiness effect and porosity have mainly focused in this paper. Furthermore, for conception and physical demonstration the entrenched parameters, like porosity parameter k, Prandtl number Pr, unsteadiness parameter S, Radiation parameter Rd, Magnetic parameter M, and Williamson fluid parameter have been discussed graphically in detail with their effect on liquid film flow.

Keywords: Applied mathematics, Computational mathematics

https://doi.org/10.1016/j.heliyon.2018.e00825

1. Introduction

The flow analysis of thin film has got important loyalty due to its enormous applications in the field of engineering and technology in several years. The field of thin film flow problems is vast and is realized in many fields, starting from the particular situation of the flow in human lungs to lubricant problems in industry. Investigating the uses of thin liquid film flow is an interesting interaction between structural mechanics, fluid mechanics, and theology. Extrusion of polymer and metal, striating of foodstuff, constant forming, elastic sheets drawing, and fluidization of the devices, exchanges, and chemical treating apparatus are several well-known uses of liquid films. In observations of these uses and applications, the study of liquid film becomes necessary for researchers to further investigate and make further development in it. Different approaches with modified geometries have been adopted by many researchers from time to time. In view of the industrial applications of thin film flow, stretching surface has become an important topic for researchers. In early days, the study of liquid film flow was limited to viscous fluids. Crane [1] is the pioneer to deliberate the flow of viscid fluid in a linear extending surface. Dandapat [2] has deliberate viscoelastic fluid flow on an extending surface with heat transfer. Wang [3] was the first one to investigate finite liquid film at a time depending stretched surface. Ushah and Sridharan [4] have investigated the flow of finite thin liquid over a time depending stretching surface. The same work is extended by Liu and Andersson [5] using numerical techniques. Aziz et al. [6] has examined the consequence of inner heat production on flow in a thin liquid film on a time depending stretching sheet. Recently, Tawade et al. [7] has reviewed the liquid flow over an unstable extending sheet with thermal radioactivity. Andersson [8] is the forerunner to investigate the flow of tinny liquid films of non-Newtonian fluids in an unsteady stretching sheet by considering the Power law model. Waris et al. [9] has studied the nanoliquid film flow over an unstable stretching sheet with varying viscosity and thermal conductivity. Andersson et al. [10], Chen [11, 12], and Wang et al. [13], have deliberated thin liquids flow using different physical configuration. Singh Megahe et al. [14] has examined tinny film flow of Casson fluid in the occurrence of irregular heat flux and viscid dissipation. Abolbashari et al. [15] work out thin film flow with entropy generation. Qasim et al. [16] has studied the Nano fluid thin film on an unstable extending surface taking Buongiorno's model.

Non-Newtonian fluids have so many types in nature as well as in artificial. Williamson fluid is one of significant subtypes between them. A number of researchers investigated Williamson fluid with different effects. Practical application has produced interest in searching the solvability of differential equation governing in flow of Non-Newtonian liquids, which have numerous uses in engineering field, applied mathematics and computer science. Many environmental and industrial systems like system of geothermal energy and system of heat exchanger design include

https://doi.org/10.1016/j.heliyon.2018.e00825

the convection flow subject to permeable medium. The adapted form of classical Darcian model is the non-Darcian porous medium, which contains the inertia and boundary topographies. The standard Darcy's law is effective under constrained range of small permeability and little velocity. Forchheimer [17] has predicted the inertia and boundary features by including a square velocity term to the countenance of Darcian velocity. Muskat [18] has entitled this term as "Forchheimer term" which is permanently operative for large Reynolds number. Dawer et al. [19] have studied fluid flow in porous media. The more current investigational and theoretical study of Sheikholeslami [20, 21, 22] on nanofluids using dissimilar phenomena, with modern application, possessions and properties with usages of diverse approaches can be studied in Tahir et al. [23] have studied flow of a nano-liquid film of maxwell fluid with thermal radiation and magneto hydrodynamic properties on an unstable stretching sheet. The stuided and application of porous media can been seen in [24, 25].

In (1992) Liao [26, 27] was the first one to investigate Homotopy Analysis method. Due to its fast convergence, many researchers Shah et al. [28, 29, 30, 31], Ishaq et al. [32], Saleem et al [33]. Hameede and Muhammad et al. [34, 35] have used this method to answer highly non-linear combined equations. Khan et al. [36, 37] have used this method for the solution of Boundary layer flow problems. Prasannakumara et al. [38] investigated Williamson nanofluid with impact of chemical reaction and nonlinear radiation embedded in a permeable sheet. Krishnamurthy et al. [39] have investigates slip flow and heat transmission of nanofluid over a porous stretching sheet with impact of nonlinear thermal radiation. Chaudhary et al. [40] has explored thermal radiation properties of fluid on the extending stretching surface. Das [41] has studied properties of thermophoresis and thermal radiation convective flow with heat transmission analysis. Muhammad et al. [35] have examined radiative flow of MHD carbon nanotubes. The more recent study about thermal radiation and can be studied in [42, 43].

In all of the discussed work, researchers consider heat and mass transmission features of Newtonian or non-Newtonian fluid at a time depended and a time independent extending surface, taking one or more physical characteristics. The main goal of this research is to investigate liquid film flow Williamson fluids over a stretched surface in the existence of magnetic field and thermal radiation. Keeping in view all these assumptions taken into the modelled problem and the similarity transformation method, the concerned PDEs are converted to non-linear ODEs, and the obtained, transformed equations are analytically solved using HAM.

2. Theory/Calculation

Consider the flow of non-Newtonian liquid film flow (considering Williamson fluid) with impact of thermal radiation over an unsteady porous stretching sheet. The

https://doi.org/10.1016/j.heliyon.2018.e00825

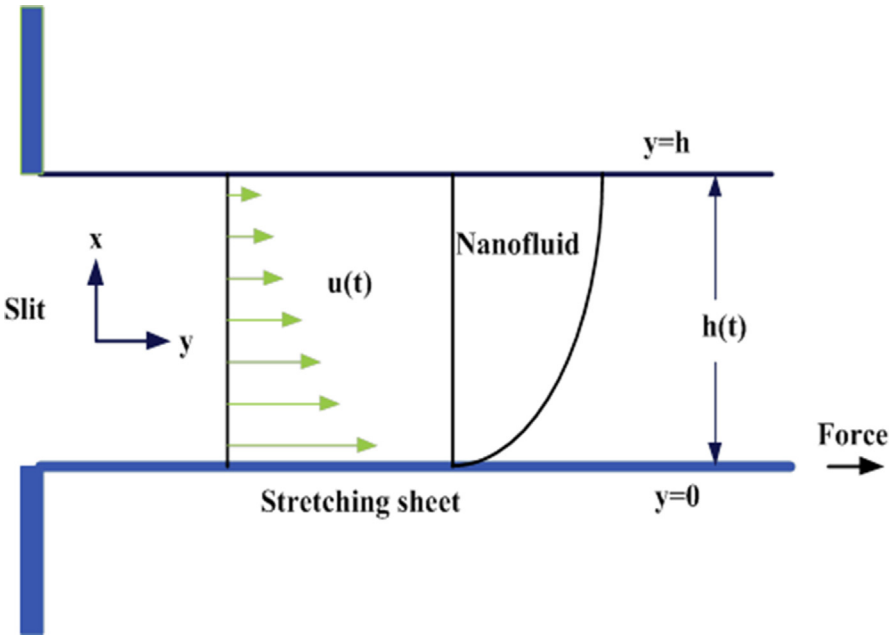

Fig. 1. Geometry of the demonstrated problems.

coordinate system is chosen in such a way that the x-axis is parallel to the slit while the y-axis is perpendicular to the surface respectively (Fig. 1). The x-axis is taken along the spreading surface with stress velocity as $\mathbf{U}_0(x,\mathrm{t}) = \frac{\varepsilon x}{1-\xi \mathrm{t}}$, where $\xi > 0$, is the stretching parameter. The heat transmission to the fluid flow and the temperature is defined as $\mathrm{T_s}(x,\mathrm{t}) = \mathrm{T}_\circ - \mathrm{T}_{ref}\left[\frac{\xi x^2}{2\upsilon}\right](1-\varepsilon \mathrm{t})^{-1.5}$, called surface temperature fluctuating with the distance x from the slit. The time dependent term $\frac{\varepsilon x^2}{\upsilon(1-\xi t)}$ can be renowned as the local Reynold number, reliant on the velocity $\mathbf{U}_0(x,t)$. Here T_0 is temperature at the slit, T_{ref} is the reference temperature such that $0 \leq \mathrm{T}_{ref} \leq \mathrm{T}_0$. The slit is fixed at the origin initially and then some exterior force is acting to stretch the slit at the rate $\frac{\varepsilon x}{1-\xi \mathrm{t}}$ in time $0 \leq \xi \leq 1$ with velocity $\mathbf{U}_0(x,t)$ is in the positive x-direction. Also $\mathrm{T}_s(x,t)$ designates the sheet temperature, reduce from T_0 at the slit in $0 \leq \xi \leq 1$.

In the interpretation of above expectations, the main leading equations are articulated as:

$$\frac{\partial u}{\partial x} + \frac{\partial v}{\partial y} = 0, \tag{1}$$

$$\left(\frac{\partial u}{\partial t}\right) + u\left(\frac{\partial u}{\partial x}\right) + v\left(\frac{\partial u}{\partial y}\right) = \frac{\mu_0}{\rho}\left[\left(\frac{\partial^2 u}{\partial y^2}\right) + \sqrt{2}\,\Gamma\left(\frac{\partial u}{\partial y}\frac{\partial^2 u}{\partial y^2}\right)\right] - \left(\frac{\upsilon\phi}{\rho k} - \frac{\sigma B_0^2}{\rho}\right)u(t), \tag{2}$$

Here in Eqs. (1) and (2) υ represents the kinematics viscosity where $\upsilon = \frac{\mu_0}{\rho}$, $\Gamma > 0$ represents the material constant of the Williamson fluid, ρ is the density of the fluid and σ denotes the electrical conductivity.

https://doi.org/10.1016/j.heliyon.2018.e00825

$$\left(\frac{\partial T}{\partial t}\right)+u\left(\frac{\partial T}{\partial x}\right)+v\left(\frac{\partial T}{\partial y}\right)=\frac{k}{\rho C_p}\left(\frac{\partial^2 T}{\partial y^2}\right)-\frac{1}{\rho C_p}\left(\frac{\partial q_r}{\partial y}\right). \tag{3}$$

Here q_r is Rosseland approximation of the radioactive heat flux and is modelled as,

$$\frac{\partial q_r}{\partial y}=-\frac{4\sigma^*}{3k^*}\frac{\partial(T^4)}{\partial y}, \tag{4}$$

Here T represents the temperature fields, σ^* is the Stefan-Boltzmann constant, K^* is the mean absorption coefficient, k is the thermal conductivity of the liquid film. Expanding T^4 using Taylor's series about T_0 as below

$$\mathrm{T}^4=\mathrm{T}_0^4+4\mathrm{T}_0^3(\mathrm{T}-\mathrm{T}_0)+6\mathrm{T}_0^2(\mathrm{T}-\mathrm{T}_0)^2+\ldots., \tag{5}$$

Neglecting the higher order terms Eq. (5)

$$\mathrm{T}^4\cong -3\mathrm{T}_0^4+4\mathrm{T}_0^3\mathrm{T}, \tag{6}$$

Inserting Eq. (6) in Eq. (4) we obtain

$$\frac{\partial q_r}{\partial y}=-\frac{16\mathrm{T}_\infty^*\sigma^*}{3k^*K^*}\frac{\partial^2\mathrm{T}^4}{\partial y^2}, \tag{7}$$

By putting Eq. (7) in Eq. (4), it reduced as

$$\frac{\partial \mathrm{T}}{\partial t}+u\frac{\partial \mathrm{T}}{\partial x}+v\frac{\partial \mathrm{T}}{\partial y}=\frac{k}{\rho C_p}\frac{\partial^2\mathrm{T}}{\partial y^2}-\frac{1}{\rho C_p}\left(\frac{16\mathrm{T}_\infty^*\sigma^*}{3K^*}\frac{\partial^2\mathrm{T}^4}{\partial y^2}\right), \tag{8}$$

The accompanying boundary conditions here in Eqs. (1) and (2)

$$\begin{aligned} &u=\mathbf{U},\ v=0,\ T=T_s,\ \text{at y}=0,\\ &\frac{\partial u}{\partial y}=\frac{\partial T}{\partial y}=0\ \text{at y}=\text{h.}, \end{aligned} \tag{9}$$

Familiarizing the dimensionless (f) variables and similarity transformations (η) to reduce Eqs. (2), (8), and (9)

$$\begin{aligned} &f(\eta)=f(\eta)=\psi(x,y,t)\left(\frac{vb}{1-at}\right)^{-\frac{1}{2}},\ \eta=\sqrt{\frac{b}{v(1-at)}}y,\ h(t)=\sqrt{\frac{v(1-at)}{b}},\\ &\theta(\eta)=T_0-T(x,y,t)\left(\frac{bx^2}{2v(1-at)^{-\frac{3}{2}}}(T_{ref})\right)^{-1} \end{aligned} \tag{10}$$

The stream function $\psi(x,y,t)$ satisfying Eq. (1), and in term of velocity components is obtained as

https://doi.org/10.1016/j.heliyon.2018.e00825

$$u = \frac{\partial \psi}{\partial y} = \frac{bx}{(1-at)} f'(\eta), v = -\frac{\partial \psi}{\partial x} = -\left[\frac{\upsilon b}{1-at}\right]^{\frac{1}{2}} f(\eta), \tag{11}$$

Using Eqs. (10) and (11) in (1), (2), (3), (4), (5), (6), Eq. (1) satisfied and the other governing equations reduced as:

$$f''' + Wef''f''' - (f')^2 - ff'' - S\left(f' + \frac{\eta}{2} f''\right) - Mf' - kf' = 0, \tag{12}$$

$$(1+Rd)\theta'' - \Pr\left(\frac{S}{2}(3\theta + \eta\theta') + 2f'\theta - \theta' f\right) = 0, \tag{13}$$

$$\begin{aligned} &f'(0) = 1, f(0) = 0, \quad \theta(0) = 1, \\ &f''(\beta) = 0, \quad \theta'(\beta) = 0, \\ &f(\beta) = \frac{S\beta}{2} \end{aligned} \tag{14}$$

After interpretation we obtained the following physical parameters as:

$$\begin{aligned} &\mathrm{S} = \frac{a}{b}, \Pr = \frac{\rho \upsilon c_p}{k} = \frac{\mu c_p}{k}, \quad \mathrm{Rd} = \frac{4\sigma T_s^3}{kk^*}, \quad We = \Gamma x \sqrt{\frac{2b^3}{\upsilon(1-at)^3}}, \\ &M = \frac{\rho B_0^2}{\rho b}(1-at), \; k == \frac{\upsilon \phi}{kb}(1-at) \end{aligned} \tag{15}$$

Here in Eq. (15) Pr signifies the Prandtl number, S used for unsteadiness Parameter, Rd represents the radiation parameter and We is a fluid material constant, M is magnetic parameter, k represents porosity parameter and all of these are defined respectively. The Skin friction is defined as

$$\mathrm{C}_f = \frac{\left(S_{xy}\right)_{y=0}}{\rho U_w^2}, \tag{16}$$

Where S_{xy} in Eq. (16) is defined as

$$S_{xy} = \mu_0 \left(\frac{\partial u}{\partial y} + \frac{\Gamma}{\sqrt{2}} \left(\frac{\partial u}{\partial y}\right)^2\right) = 0 \tag{17}$$

The dimensionless form of Eq. (17)

$$\mathrm{C}_f \sqrt{\mathrm{Re}_x} = f''(0) + W_e (f'')^2(0). \tag{18}$$

Where R_{ex} in Eq. (18) is called local Reynolds number. The Nusselt number is defined as $Nu = \frac{\delta Q_w}{\widehat{k}(T-T_0)}$, in which Q_w is the heat flux, where $Q_w = -\widehat{k}\left(\frac{\partial T}{\partial y}\right)_{\eta=0}$, Here the dimensionless form of Nu is obtained in Eq. (19) below

$$Nu = -\left(1 + \frac{4}{3} Rd\right)\Theta'(0), \tag{19}$$

https://doi.org/10.1016/j.heliyon.2018.e00825

3. Methodology

For solution of the problem we implement the Homotopy Analysis Method to fin the solution of Eqs. (12) and (13), consistent with the boundary constraints (14). The solutions enclosed the secondary parameters $\hbar$, which standardize and switches to the combination of the solutions. Initial solution of Eqs. (12) and (13) are given in Eq. (20)

$$f_0(\eta) = \eta,\ \theta_0(\eta) = 1, \tag{20}$$

The linear operators can be chosen as

$$L_f(f) = \frac{d^4 f}{d\eta^4},\ \mathrm{L}_\theta(\theta) = \frac{d^2\theta}{d\eta^2}. \tag{21}$$

The differential operators in (21) content are defined as

$$\begin{aligned} &L_f\left(\psi_1 + \psi_2\eta + \psi_3\eta^2 + \psi_4\eta^3\right) = 0, \\ &L_\theta(\psi_5 + \psi_6\eta) = 0. \end{aligned} \tag{22}$$

Here in Eq. (22) $\sum_{i=1}^{6}\psi_i$, where $i = 1, 2, 3...$ are arbitrary constants. Expressing $q\in$ $[0 \quad 1]$ as an entrenching parameter with associate parameters $\hbar_f$ and $\hbar_\theta$ where $\hbar \neq 0$. Then the problem in case of zero order deform to the following form

$$(1-q)L_f\left(\widehat{f}(\eta,q) - f_0(q)\right) = q\hbar_f N_f\left(\widehat{f}(\eta,q), \widehat{g}(\eta,q)\right), \tag{23}$$

$$(1-q)L_\theta\left(\widehat{\theta}(\eta,q) - \theta_0(\eta)\right) = q\hbar_\theta N_\theta\left(\widehat{f}(\eta,q), \widehat{g}(\eta,q), \widehat{\theta}(\eta,q)\right). \tag{24}$$

The subjected boundary conditions for Eqs. (23) and (24) are obtained in Eq. (25)

$$\begin{aligned} &f(0) = 0, f'(0) = 1, f(\beta) = \frac{S\beta}{2}, f''(\beta) = 0, \\ &\theta(0) = \theta'(\beta) = 0. \end{aligned} \tag{25}$$

The resultant nonlinear operators are

$$\begin{aligned} &N_f\left(f(\eta;q), \widehat{\theta}(\eta;q)\right) = f_{\eta\eta\eta} + Weff_{\eta\eta} - f_\eta f_\eta - ff_{\eta\eta} \\ &-S\left[f_\eta + \frac{\eta}{2}f_{\eta\eta}\right] - Mf_\eta - kf_\eta, \end{aligned} \tag{26}$$

Using the Taylor's series expansion to expand $\mathrm{f}(\eta;q)$ and $\theta(\eta;q)$ in Eq. (26) in term of q we get

https://doi.org/10.1016/j.heliyon.2018.e00825

$$f(\eta,q) = f_0(\eta) + \sum_{i=1}^{\infty} f_i(\eta),$$
$$\theta(\eta,q) = \theta_0(\eta) + \sum_{i=1}^{\infty} \theta_i(\eta), \tag{27}$$

Where

$$f_i(\eta) = \frac{1}{i!}\widehat{f}_{\eta}(\eta,q)\Big|_{q=0},\ \theta_i(\eta) = \frac{1}{i!}\widehat{\theta}_{\eta}(\eta,q)\Big|_{q=0}. \tag{28}$$

Differentiating Zeroth order Eqs. (27) and (28) ith time we obtained the ith order deformation equations with respect to q dividing by $i!$ and then inserting $q = 0$. So i^{th} order deformation equations

$$L_f(f_i(\eta) - \xi_i f_{i-1}(\eta)) = h_f \Re_i^f(\eta),$$
$$L_\theta(\theta_i(\eta) - \xi_i \theta_{i-1}(\eta)) = h_\theta \Re_i^\theta(\eta). \tag{29}$$

The resultant boundary conditions for Eq. (29) are

$$f_i(0) = f_i'(0) = f_i(\beta) = \frac{S\beta}{2},\ f_i''(\beta) = 0,$$
$$\theta_i(0) = 0, \theta_i(\beta). \tag{30}$$

$$R_i^f(\eta) = f_{i-1}'''(\eta) + We\sum_{j}^{i-1} f_{i-1-j}'' f_j''' - \sum_{j=0}^{i-1} f_{i-1-j}' f_j' - f_{i-1-j} f_j'' - S\left[f_{i-1}'(\eta) + \frac{\eta}{2} f_{i-1}''\right]$$
$$- M f_{i-1}' - k f_{i-1}', \tag{31}$$

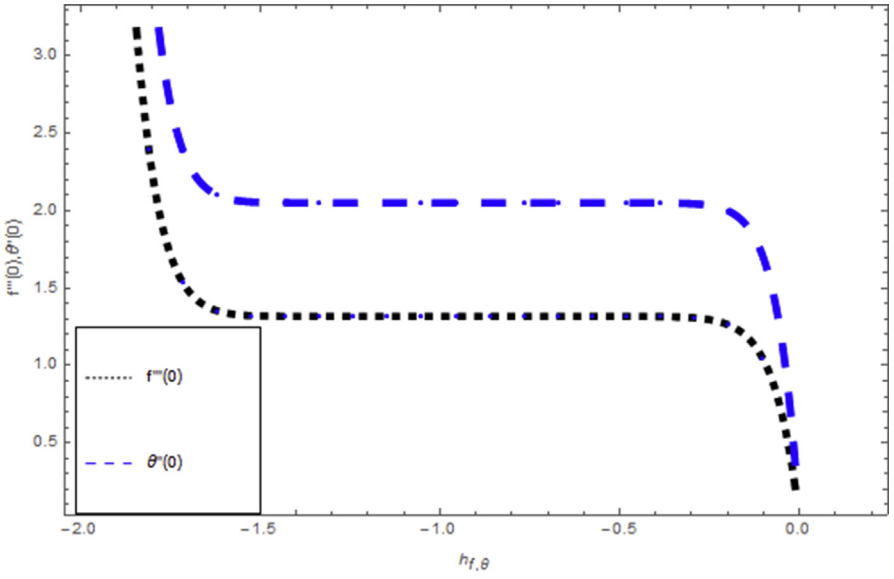

Fig. 2. Combined h curves of $f(\eta)$ and $\theta(\eta)$ at 12^{th} order approximation.

https://doi.org/10.1016/j.heliyon.2018.e00825

$$R_k^{\theta}(\eta) = \theta''_{i-1}(\eta) - \Pr\left[\sum_{j=0}^{i-1} f_{i-1-j}\theta'_j - 2\sum_{j=0}^{i-1} f'_{i-1-j}\theta_j - \left(\frac{S}{2}\left(3\theta_{i-1} + \eta\theta'_{i-1}\right)\right)\right]. \quad (32)$$

Where

$$\xi_i = \begin{cases} 1, & \text{if } q > 1 \\ 0, & \text{if } q \leq 1 \end{cases} \quad (33)$$

Hence (30), (31), (32), (33) are the final simplified equitation's.

Table 1. Convergence of $f''(0)$ *and* $\Theta'(0)$ by HAM method when $We = 0.2,\ \beta = \mathrm{Rd} = \Pr = S = \mathrm{k} = 0.1, \mathrm{M} = 0.5.$

Solution Approximations	$f''(0)$	$\Theta'(0)$
1	−1.90218	−0.24761
2	−1.90259	−0.214609
3	−1.90267	−0.219032
4	−1.90268	−0.218439
5	−1.90269	−0.218519
6	−1.90269	−0.218508
7	−1.90269	−0.218510
8	−1.90269	−0.218509
9	−1.90269	−0.218509

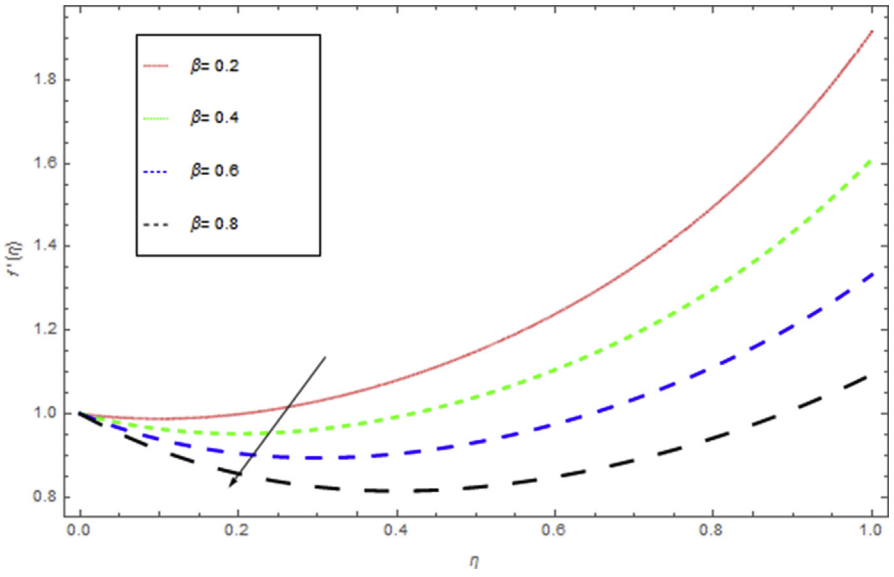

Fig. 3. The influence of β on $f(\eta)$ when $h = -1.9, S = 0.5, M = 1, k = 0.4, We = 0.4.$

https://doi.org/10.1016/j.heliyon.2018.e00825

4. Analysis

Here our interest is to analyze analytical solution of obtaining system of ordinary differential equations by Homotopy Analysis Method. When the series solution of the velocity and temperature profile are computed by HAM, the assisting parameters h_f, h_θ seems which responsible for adjusting of convergence. In the acceptable region of h, h-curves of $f''(0)$ and $\theta'(0)$ are plotted in Fig. 2, displaying the valid region.

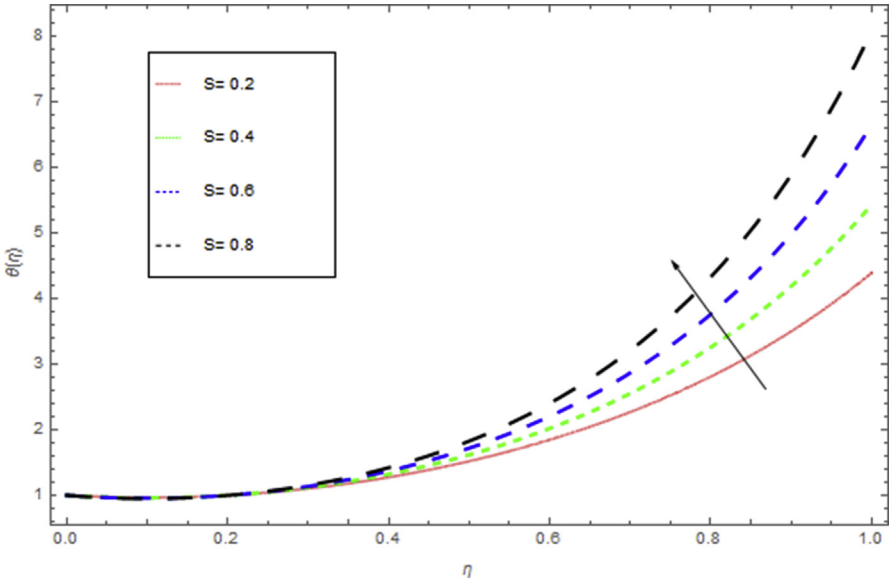

Fig. 4. The influence of S on $f(\eta)$ when $\mathrm{h} = 1.2, \beta = We = 0.5, k = 0.4, M = 1$.

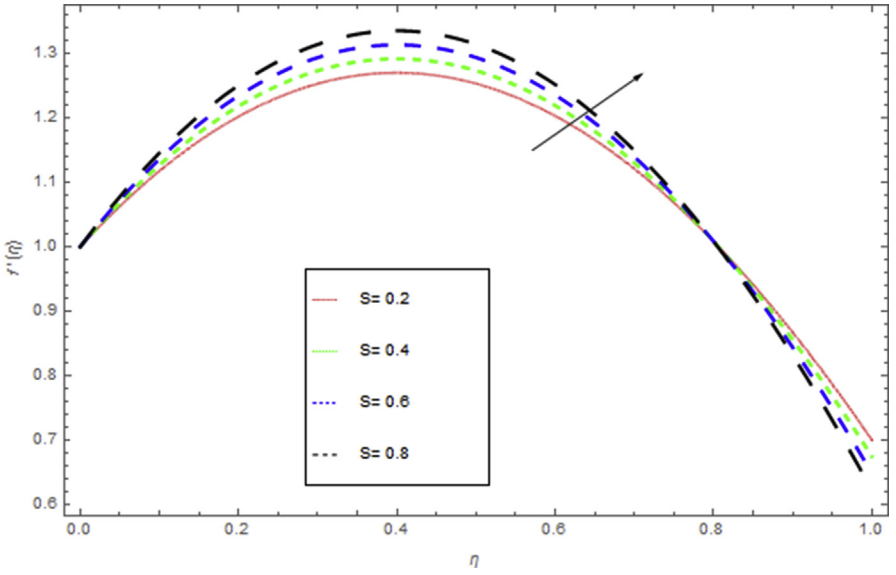

Fig. 5. The influence of S on $\theta(\eta)$ when $\mathrm{Rd} = 0.3, \mathrm{h} = 1.5, \beta = 0.1, We = 0.5, k = 0.4, M = 1, \mathrm{Pr} = 0.8$.

https://doi.org/10.1016/j.heliyon.2018.e00825

Table 1 displays the numerical values of HAM solutions showing that homotopy analysis technique is a speedily convergent technique.

5. Results and discussion

The current research has been conceded out to study the flow of Williamson liquid film flow in a time dependent starching sheet with the impact of MHD and thermal radiation. The determination of this section is to examine the physical consequences

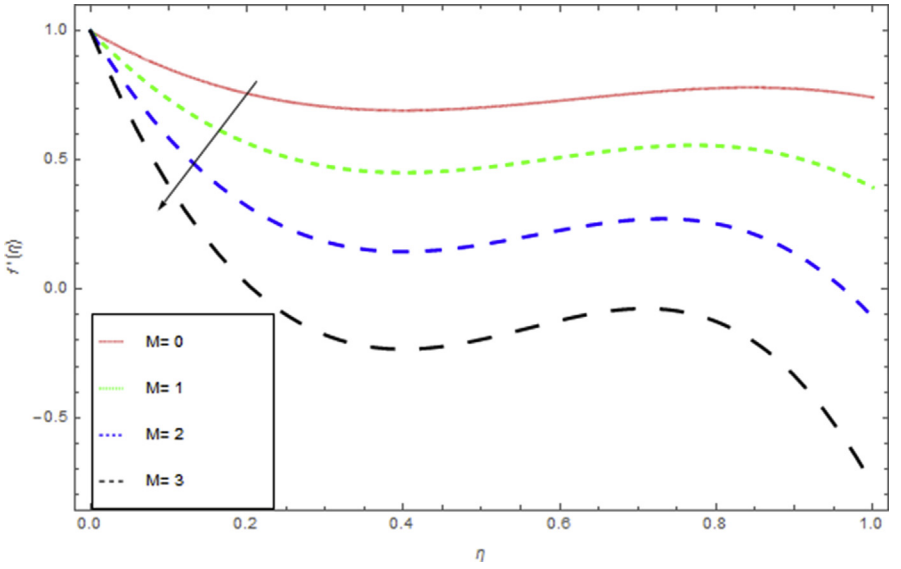

Fig. 6. The influence of M on $f(\eta)$ when h $= 1.3, \beta = We = 0.5, k = 0.4, S = 0.2$.

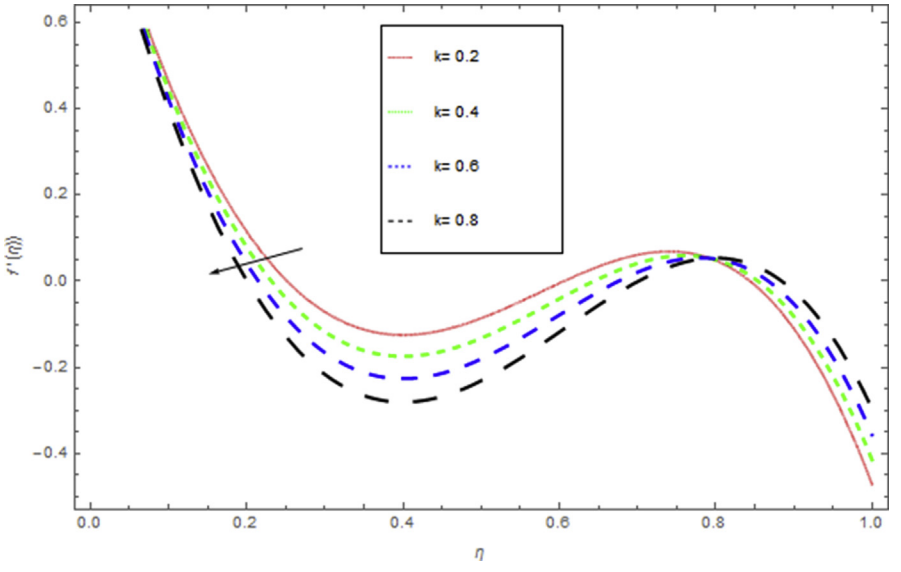

Fig. 7. The influence of k on $f(\eta)$ when h $= 0.9, \beta = 0.4, We = 0.6, S = 0.4, M = 1$.

https://doi.org/10.1016/j.heliyon.2018.e00825

of different embedding parameters on the velocity $f(\eta)$ and temperature $\Theta(\eta)$ profiles, which are illustrated in Figs. 3, 4, 5, 6, 7, 8, 9, and 10. Fig. 3 demonstrates the influence of the liquid film thickness β throughout the flow motion. Increasing β decreases the flow velocity of the liquid film. Actually fluid film produces opposition to the film flow and reduces $f(\eta)$ with higher values of β. Fig. 4 determines the behaviour of the parameter S on the $f(\eta)$. It is perceived that $f(\eta)$ directly varies with unsteadiness parameter S. Increasing S rise the fluid motion. It is perceived that

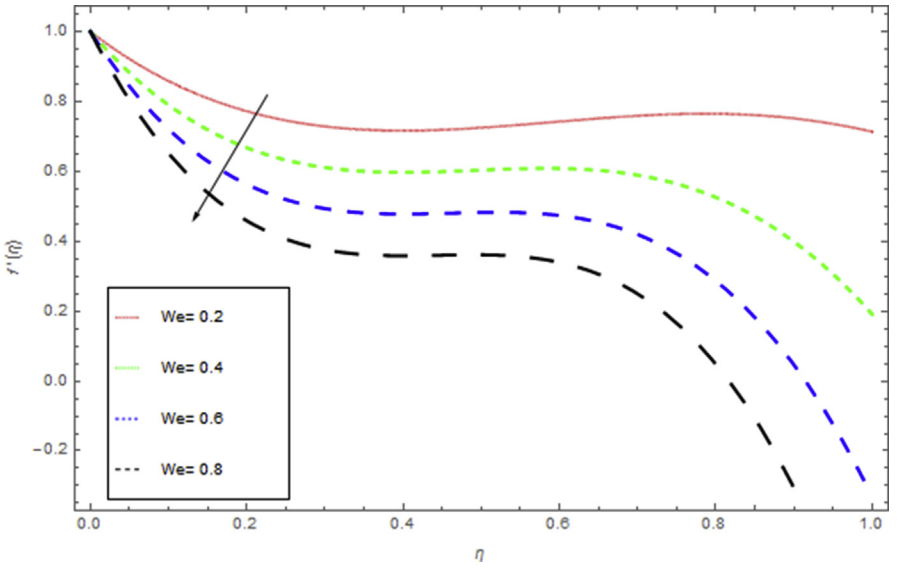

Fig. 8. The influence of We on $f(\eta)$ when $\mathrm{h} = -1.2, \beta = S = 0.5, k = 0.4, M = 0.6$.

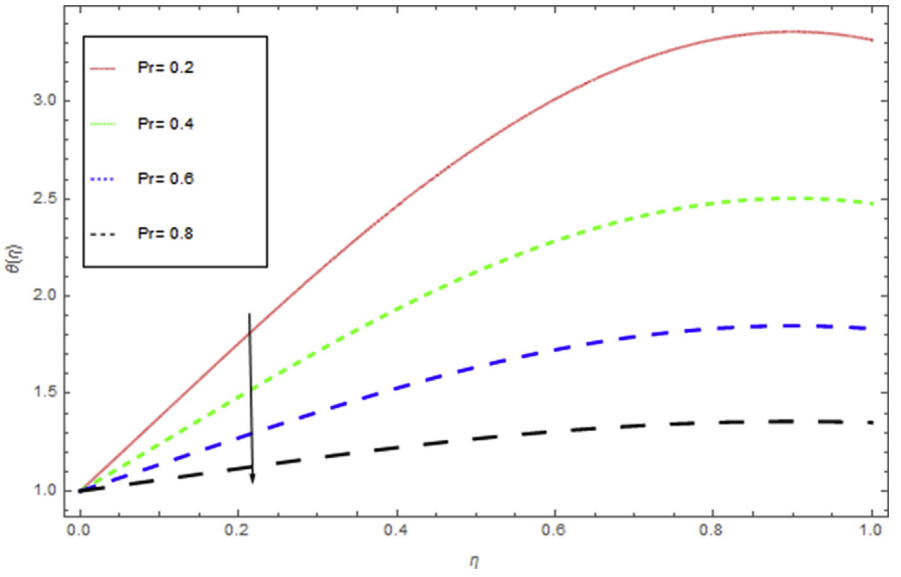

Fig. 9. The influence of Pr on $\theta(\eta)$ when $\mathrm{Rd} = 0.5, \mathrm{h} = -1.5, \beta = 0.4, We = 0.5, k = 0.6, M = 0.5, S = 0.4$.

https://doi.org/10.1016/j.heliyon.2018.e00825

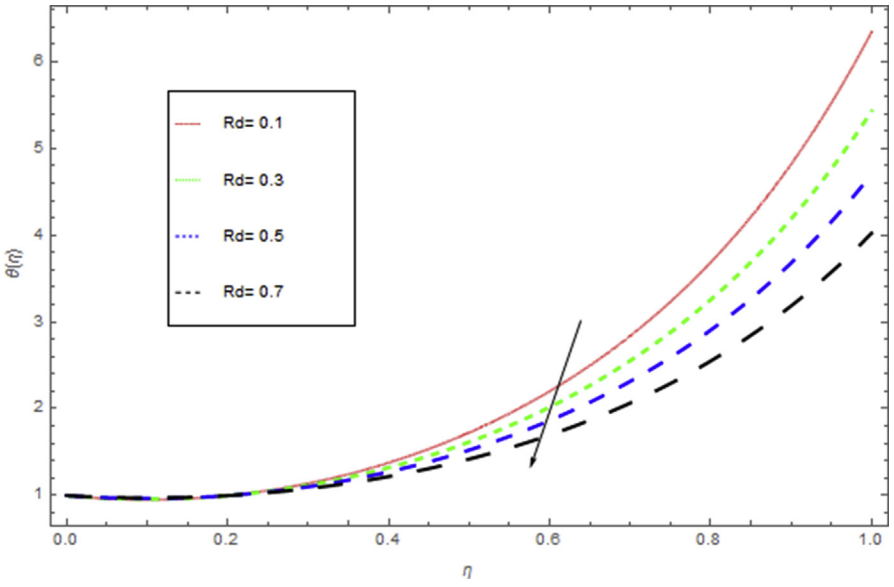

Fig. 10. The influence of Rd on $\theta(\eta)$ when $\Pr = 0.5, \mathrm{h} = -1.5, \beta = 0.4, We = 0.5, k = 0.6, M = 0.5, S = 0.4$.

Table 2. The Skin friction coefficient for dissimilar values of Re, Kr, β and γ when $S = 0.4$.

M	**Pr**	***Rd***	**k**	**Tawade et al [1] results $\theta(\beta)$**	**Present results $\theta(\beta)$**
0.0	0.1	1.0	0.1	0.257696	0.223456
1.0				0.420739	0.432111
2.0				0.526782	0.712351
5.0				0.695757	1.023001
1.0	0.01			1.030899	1.625341
	0.1			0.931433	1.236540
	1.0			0.420739	0.988872
	5.0			0.011137	0.566100
	1.0	0.0		0.227566	0.222109
		1.0		0.420739	0.432091
		3.0		0.715871	0.674109
		5.0		0.826899	0.992221
		1.0	0.1	0.190930	0.011236
			0.2	0.223926	0.227634
			0.3	0.250515	0.537000
			0.4	0.281804	0.719273
				0.340312	1.200235

https://doi.org/10.1016/j.heliyon.2018.e00825

solution depended on the unsteadiness parameter S, the solution exist only when $S \in [0 \quad 0]$. Fig. 5 shows the influence of the unsteadiness parameter S on the $\theta(\eta)$. It is perceived that $\theta(\eta)$ directly varies with unsteadiness parameter S. Increasing S rises the temperature and as a result increase the kinetic energy of the fluid, so the liquid film motion increases. Fig. 6 describes the characteristics of the magnetic strength M. When the magnetic strength rises on the sheet surface through the fluid flow, the internal fluid resistance increases, which causes reduction in the velocity field. The reason for this phenomenon is the enhancement of magnetic field to a fluid which crops a conflict force called the Lorentz force. This force carries the reduction in the motion of the fluid. Fig. 7 shows the impact of porosity parameter k on $f(\eta)$, which has an domineering eccentric in the flow motion. It is perceived that the augmented value of k rises the porous space which makes resistance in the motion and reduces it speed. The motion of the fluid under the influence of We is deliberated in Fig. 8. The velocity $f(\eta)$ decreases with rising values of We. In fact, increase in relaxation time produces resistance force and eventually declines the fluid velocity. The impact of Pr on $\Theta(\eta)$, is shown in Fig. 9. It is clear that temperature field declines with higher numbers of Pr and increases for small values of

Table 3. Wall temperature gradient $\Theta'(0)$ verses various value of embedded parameters when $h = 0.1$.

Rd	***β***	**Pr**	***S***	$\Theta'(\mathbf{0})$
0.0	0.2	1.0	0.2	0.682385
0.5				0.541422
1.0				0.440569
2.0				0.311380
1.0	0.1			0.411411
	0.2			0.321022
	0.3			0.300420
	0.4			0.291420
	0.5			0.111427
	0.1	0.1		0.411420
		0.5		0.371420
		1.5		0.182285
		5.0		0.011422
		10		0.000569
		1.0	0.2	0.411420
			0.4	0.612427
			0.6	0.891428
			0.8	1.500987
			1.0	2.087651

https://doi.org/10.1016/j.heliyon.2018.e00825

Table 4. The effects of dissimilar values of M, k, β and We on Skin friction coefficient.

M	k	β	We	$-(C_f \mathrm{Re}_x)^{\frac{1}{2}}$
0.1	0.5	1.0	1.5	3.33027
0.5				2.94882
1.0				2.64208
1.5	0.1			4.33999
	0.5			4.32157
	1.0			4.26897
	1.5	0.1		5.64227
		0.5		5.44576
		1.0		4.89911
		1.5	0.1	4.12743
			0.5	4.35772
			1.0	5.13048
			1.5	5.91612

Pr. Fig. 10 shows the influence of radiation parameter Rd on temperature profile. When we increase thermal radiation parameter Rd, then it is perceived that it augments the temperature in the fluid layer. This increase leads to drop in the rate of cooling for thin film flow.

The numerical values of the surface temperature $\theta(\beta)$ for different value of M, Rd and k are given in Table 2. It is observed that the increasing values of M, Rd and k increase the surface temperature $\theta(\beta)$, where opposite effect is found for Pr, that is the large value of Pr reduces the surface temperature $\theta(\beta)$. The numerical values of the heat flux $\Theta'(0)$ for dissimilar values of embedded parameters Rd, β, Pr, S have been shown in Table 3. It is perceived that larger values of thermal radiation Rd, β and Pr decrease the wall temperature and S increases the wall temperature gradient $\Theta'(0)$. The numerical values of M, k, β and We on skin friction C_f are given in Table 4. From this table it is obvious that high values of M, k and β decrease C_f while increasing We increases skin friction.

6. Conclusion

The conclusion of the present work is mainly focused on the behaviour of embedded parameters and solutions of the obtained results. The central concluded points are:

- Thermal boundary layer thickness reduces with rise of radiation parameter Rd So, Nusselt number Nu rises with rise of radiation parameter Rd.

https://doi.org/10.1016/j.heliyon.2018.e00825

- The increasing values of M, Rd and k increase the surface temperature $\theta(\beta)$, where opposite effect is found for Pr, that is the large values of Pr reduce the surface temperature $\theta(\beta)$.
- Increasing k reduce the flow of thin films.
- For skin friction C_f it is found that it increases when the viscosity parameter R is decreased.
- It is notice that the strong magnetic field reduce the velocity he liquid films.
- It is also concluded that liquid film flow is affected by the Lorentz's force.

Declarations

Author contribution statement

Zahir Shah, Ebenezer Bonyah, Saeed Islam, Waris Khan, Mohammad Ishaq: Conceived and designed the analysis; Analyzed and interpreted the data; Contributed analysis tools or data; Wrote the paper.

Funding statement

This research did not receive any specific grant from funding agencies in the public, commercial, or not-for-profit sectors.

Competing interest statement

The authors declare no conflict of interest.

Additional information

No additional information is available for this paper.

References

[1] L.J. Crane, Flow past a stretching plate, Angrew. Math. Phys. 21 (1970) 645−647.

[2] B.S. Dandapat, A.S. Gupta, Flow and heat transfer in a viscoelastic fluid over a stretching sheet, Int. J. Nonlinear Mech. 24 (1989) 215−219.

[3] C.Y. Wang, Liquid film on an unsteady stretching surface, Q. Appl. Math. 48 (1990) 601−610. jstor.org/stable/43637666.

[4] R. Usha, R. Sridharan, On the motion of a liquid film on an unsteady stretching surface, ASME Fluids Eng. 150 (1993) 43−48.

 https://doi.org/10.1016/j.heliyon.2018.e00825

[5] I.C. Liu, I.H. Andersson, Heat transfer in a liquid film on an unsteady stretching sheet, Int. J. Therm. Sci. 47 (2008) 766–772.

[6] R.C. Aziz, I. Hashim, A.K. Alomari, Thin film flow and heat transfer on an unsteady stretching sheet with internal heating, Meccanica 46 (2011) 349–357.

[7] L. Tawade, M. Abel, P. GMetri, A. Koti, Thin film flow and heat transfer over an unsteady stretching sheet with thermal radiation, internal heating in presence of external magnetic field, Int. J. Adv. Appl. Math. Mech. 3 (2016) 29–40.

[8] H.I. Andersson, J.B. Aarseth, N. Braud, B.S. Dandapat, Flow of a power-law fluid film on an unsteady stretching surface, J. Non Newtonian Fluid Mech. 62 (1996) 1–8.

[9] K. Waris, T. Gul, M. Idrees, S. Islam, I. Khan, L.C.C. Dennis, Thin film Williamson nanofluid flow with varying viscosity and thermal conductivity on a time-dependent stretching sheet, Appl. Sci. 6 (2016) 334.

[10] H.I. Anderssona, J.B. Aarseth, B.S. Dandapatb, Heat transfer in a liquid film on an unsteady stretching, Int. J. Heat Mass Transf. 43 (2000) 69–74.

[11] C.H. Chen, Heat transfer in a power-law liquid film over a unsteady stretching sheet, Heat Mass Transf. 39 (2003) 791–796.

[12] C.H. Chen, Effect of viscous dissipation on heat transfer in a non-Newtonian liquid film over an unsteady stretching sheet, J. Non Newtonian Fluid Mech. 135 (2006) 128–135.

[13] C. Wang, L. Pop, Analysis of the flow of a power-law liquid film on an unsteady stretching surface by means of homotopy analysis method, J. Non Newtonian Fluid Mech. 138 (2006) 161–172.

[14] A.M. Megahe, Effect of slip velocity on Casson thin film flow and heat transfer due to unsteady stretching sheet in presence of variable heat flux and viscous dissipation, Appl. Math. Mech. Engl. Ed. 36 (10) (2015) 1273–1284.

[15] M.H. Abolbashari, N. Freidoonimehr, M.M. Rashidi, Analytical modeling of entropy generation for Casson nano-fluid flow induced by a stretching surface, Adv. Powder Technol. 262 (2015) 542–552.

[16] M. Qasim, Z.H. Khan, R.J. Lopez, W.A. Khan, Heat and mass transfer in nanofluid thin film over an unsteady stretching sheet using Buongiorno's model, Eur. Phys. J. Plus 131 (2016) 16.

https://doi.org/10.1016/j.heliyon.2018.e00825

[17] P. Forchheimer, Wasserbewegung durch boden, Z. Ver D Ing 45 (1901) 1782−1788.

[18] M. Muskat, The Flow of Homogeneous Fluids through Porous media, 1946. Edwards, MI.

[19] A. Dawar, Z. Shah, M. Idress, W. Khan, S. Islam, T. Gul, Impact of thermal radiation and heat source/sink on eyring−powell fluid flow over an unsteady oscillatory porous stretching surface, Math. Comput. Appl. 23 (2018) 20.

[20] M. Sheikholeslami, Influence of magnetic field on nanofluid free convection in an open porous cavity by means of Lattice Boltzmann method, J. Mol. Liq. 234 (2017) 364.

[21] M. Sheikholeslami, Numerical simulation of magnetic nanofluid natural convection in porous media, Phys. Lett. A 381 (2017) 494−503.

[22] M. Sheikholeslami, Numerical study of heat transfer enhancement in a pipe filled with porous media by axisymmetric TLB model based on GPU, Eur. Phys. J. Plus 129 (2014) 248.

[23] Fareesa Tahir, Taza Gul, Saeed Islam, Zahir Shah, Aurangzeb Khan, Waris Khan, Liaqat Ali, Muradullah, Flow of a nano-liquid film of maxwell fluid with thermal radiation and magneto hydrodynamic properties on an unstable stretching sheet, J. Nanofluids 6 (2017) 1−10.

[24] K. Vafai, Porous Media: Applications in Biological Systems and Biotechnology, CRC Press, 2010, p. 632.

[25] D. Nield, A. Bejan, A Convection in Porous Media, fourth ed., Springer, New York, 2013, p. 1268.

[26] S.J. Liao, The Proposed Homotopy Analysis Method for the Solution of Nonlinear Problems (Ph.D. thesis), Shanghai Jiao Tong University, 1992.

[27] S.J. Liao, On the analytic solution of magnetohydrodynamic flows of non-Newtonian fluids over a stretching sheet, J. Fluid Mech. 488 (2003) 189−212.

[28] Z. Shah, S. Islam, T. Gul, E. Bonyah, M.A. Khan, Three dimensional third grade nanofluid flow in a rotating system between parallel plates with Brownian motion and thermophoresis effects, Res. Phys. 10 (2018) 36−45.

[29] Z. Shah, T. Gul, A.M. Khan, I. Ali, S. Islam, Effects of hall current on steady three dimensional non-Newtonian nanofluid in a rotating frame

 https://doi.org/10.1016/j.heliyon.2018.e00825

with brownian motion and thermophoresis effects, J. Eng. Technol. 6 (2017) 280−296.

[30] Z. Shah, S. Islam, H. Ayaz, S. Khan, Radiative heat and mass transfer analysis of micropolar nanofluid flow of Casson fluid between two rotating parallel plates with effects of Hall current, ASME J. Heat Transf. (2018).

[31] Z. Shah, S. Islam, T. Gul, E. Bonyah, M.A. Khan, The electrical MHD and hall current impact on micropolar nanofluid flow between rotating parallel plates, Res. Phys. 9 (2018) 1201−1214.

[32] M. Ishaq, G. Ali, Z. Shah, S. Islam, S. Muhammad, Entropy generation on nanofluid thin film flow of eyring−powell fluid with thermal radiation and MHD effect on an unsteady porous stretching sheet, Entropy 20 (2018) 412.

[33] Saleem Nasir, Saeed Islam, Taza Gul, Zahir Shah, Muhammad Altaf Khan, Waris Khan, Aurang Zeb Khan, Saima Khan, Three-dimensional rotating flow of MHD single wall carbon nanotubes over a stretching sheet in presence of thermal radiation, Appl. Nanosci. (2018) 1−18.

[34] H. Hammed, M. Haneef, Z. Shah, S. Islam, W. Khan, S. Muhammad, The combined magneto hydrodynamic and electric field effect on an unsteady Maxwell nanofluid flow over a stretching surface under the influence of variable heat and thermal radiation, Appl. Sci. 8 (2018) 160.

[35] S. Muhammad, G. Ali, Z. Shah, S. Islam, S.A. Hussain, The rotating flow of magneto hydrodynamic carbon nanotubes over a stretching sheet with the impact of non-linear thermal radiation and heat generation/absorption, Appl. Sci. 8 (4) (2018) 482.

[36] N.A. Khan, S. Khan, F. Riaz, Boundary layer flow of Williamson fluid with chemically reactive species using scalin transformation and homotopy analysis method, Math. Sci. Lett. 3 (3) (2014) 199−205.

[37] N.A. Khan, N. Sultan, homogeneous-heterogeneous reactions in an eyring-powell, fluid over a stretching sheet in a porous medium, Spec. Top. Rev. Porous Med. 7 (1) (2016) 15−25.

[38] B.C. Prasannakumara, B.J. Gireesha, Rama S.R. Gorla, M.R. Krishnamurthy, Effects of chemical reaction and nonlinear thermal radiation on Williamson nanofluid slip flow over a stretching sheet embedded in a porous medium, J. Aerosp. Eng. 29 (5) (2016).

https://doi.org/10.1016/j.heliyon.2018.e00825

[39] S. Mukhopadhyay, K. Bhattacharyya, Unsteady flow of a Maxwell fluid over a stretching surface in presence of chemical reaction, J. Egypt. Math. Soc. 20 (2012), 470, 229−234.

[40] S. Chaudhary, S. Singh, S. Chaudhary, Thermal radiation effects on MHD Boundary layer flow over an exponentially stretching surface, Sci. Res. Publ. Appl. Math. 6 (2015) 295−303.

[41] K. Das, Effects of thermophoresis and thermal radiation on MHD mixed convective heat and mass transfer flow, Afr. Math. 24 (2012) 511−524. Union and Springer-Verlag.

[42] A. Ali, M. Sulaiman, S. Islam, Z. Shah, E. Bonyah, Three-dimensional magnetohydrodynamic (MHD) flow of Maxwell nanofluid containing gyrotactic micro-organisms with heat source/sink, AIP Adv. 8 (2018), 085303.

[43] M. Sheikholeslami, CVFEM for magnetic nanofluid convective heat transfer in a porous curved enclosure, Eur. Phys. J. Plus 131 (2016) 413.

https://doi.org/10.1016/j.heliyon.2018.e00825